Deficiency of caspase recruitment domain family, member 11 (CARD11), causes profound combined immunodeficiency in human subjects

Polina Stepensky, MD,[a]* Baerbel Keller, MSc,[b]* Mary Buchta,[b] Anne-Kathrin Kienzler, MSc,[b] Orly Elpeleg, MD,[c] Raz Somech, MD, PhD,[d] Sivan Cohen, MSc,[e] Idit Shachar, PhD,[e] Lisa A. Miosge, PhD,[f] Michael Schlesier, PhD,[b,g] Ilka Fuchs, MSc,[b] Anselm Enders, MD,[h] Hermann Eibel, PhD,[b] Bodo Grimbacher, MD,[b] and Klaus Warnatz, MD[b] *Jerusalem, Tel Aviv, and Rehovot, Israel, Freiburg, Germany, and Canberra, Australia*

Background: Profound combined immunodeficiency can present with normal numbers of T and B cells, and therefore the functional defect of the cellular and humoral immune response is often not recognized until the first severe clinical manifestation. Here we report a patient of consanguineous descent presenting at 13 months of age with hypogammaglobulinemia, *Pneumocystis jirovecii* pneumonia, and a suggestive family history.

Objective: We sought to identify the genetic alteration in a patient with combined immunodeficiency and characterize human caspase recruitment domain family, member 11 (CARD11), deficiency.

Methods: Molecular, immunologic, and functional assays were performed.

Results: The immunologic characterization revealed only subtle changes in the T-cell and natural killer cell compartment, whereas B-cell differentiation, although normal in number, was distinctively blocked at the transitional stage. Genetic evaluation revealed a homozygous deletion of exon 21 in *CARD11* as the underlying defect. This deletion abrogated protein expression and activation of the canonical nuclear factor κB (NF-κB) pathway in lymphocytes after antigen receptor or phorbol 12-myristate 13-acetate stimulation, whereas CD40 signaling in B cells was preserved. The abrogated activation of the canonical NF-κB pathway was associated with severely impaired upregulation of inducible T-cell costimulator, OX40, cytokine production, proliferation of T cells, and B cell–activating factor receptor expression on B cells.

Conclusion: Thus in patients with CARD11 deficiency, the combination of impaired activation and especially upregulation of inducible T-cell costimulator on T cells, together with severely disturbed peripheral B-cell differentiation, apparently leads to a defective T-cell/B-cell cooperation and probably germinal center formation and clinically results in severe immunodeficiency. This report discloses the crucial and nonredundant role of canonical NF-κB activation and specifically CARD11 in the antigen-specific immune response in human subjects. (J Allergy Clin Immunol 2013;131:477-85.)

Key words: *CARD11, human, combined immunodeficiency, hypogammaglobulinemia, profound combined immunodeficiency disorder, transitional B cell, nuclear factor κB, B cell-activating factor receptor, inducible T-cell costimulator, germinal center*

Combined immunodeficiency disorders (CIDs) affecting the cellular and humoral immune response in human subjects predispose patients to common bacterial and opportunistic infections. Severe forms (severe combined immunodeficiency) present in the first year of life and are caused by genetic defects affecting either the recombination of the antigen receptor or receptors of essential cytokines.[1] In recent years, several less severe forms of CID have been discovered, presenting later in life with opportunistic infections or alterations of T-cell homeostasis.[2] Although some of these patients have hypomorphic mutations of known severe combined immunodeficiency–associated genes, increasingly, new defects are discovered, altering the signaling of the T-cell receptor (TCR) or B-cell receptor (BCR) without affecting T- and B-cell numbers but affecting their function. Thus CD3γ deficiency often presents with normal T- and B-cell counts.[3] Abrogation of TCR-induced calcium response in Orai1-deficient[4] or stromal interaction molecule 1 (STIM1)–deficient[5] children permits normal differentiation of T and B cells but not their antigen-specific response. Other defects preferentially affect T-cell subpopulations, whereas total T-cell counts can be normal.[6-8] Therefore key signaling molecules downstream of the antigen receptors are prime candidates underlying profound combined immunodeficiency disorders (pCIDs).

From [a]Pediatric Hematology-Oncology and Bone Marrow Transplantation, Hadassah Hebrew University Medical Center, Jerusalem; [b]the Centre of Chronic Immunodeficiency (CCI), University Medical Center Freiburg and University of Freiburg; [c]the Monique and Jacques Roboh Department of Genetic Research, Hadassah, Hebrew University Medical Center, Jerusalem; [d]the Pediatric Department and Immunology Service, Jeffrey Modell Foundation (JMF) Center, Edmond and Lily Safra Children's Hospital, Sheba Medical Center, Tel Hashomer, the Sackler Faculty of Medicine, Tel Aviv University, Tel Aviv; [e]the Immunology Department, Weizmann Institute of Science, Rehovot; [f]the Department of Immunology, John Curtin School of Medical Research, Australian National University, Canberra; [g]the Division of Rheumatology and Clinical Immunology, University Medical Center Freiburg; and [h]the Ramaciotti Immunization Genomics Laboratory, Department of Immunology, John Curtin School of Medical Research, Australian National University, Canberra.

*These authors contributed equally to this work.

Supported by Deutsche Forschungsgemeinschaft Grant SFB 620 (to K.W.) and by the Federal Ministry of Education and Research (BMBF 01 EO0803, to K.W., H.E., and B.G.). P.S. was supported by a Dahlia Greidinger Cancer Research Fund. A.E. was supported by a Major Initiative Award from the Clive and Vera Ramaciotti Foundation and a Career Development Fellowship from the NHMRC (APP1035858).

Disclosure of potential conflict of interest: B. Keller has received grants from Bundesministerium fur Bildung und Forschung (BMBF). B. Grimbacher has received grants from the Federal Ministry of Education and Research. K. Warnatz has received grants from BMBF and Baxter, and has received payment for lectures, including service on speakers' bureaus, from Baxter, GlaxoSmithKline, CSL Behring, and Pfizer. I. Fuchs has received grants from BMBF. The rest of the authors declare that they have no relevant conflicts of interest.

Received for publication September 15, 2012; revised November 26, 2012; accepted for publication November 29, 2012.

Corresponding author: Klaus Warnatz, MD, Centre of Chronic Immunodeficiency, University Medical Center, Freiburg, Breisacher Str. 117, 79106 Freiburg, Germany. E-mail: klaus.warnatz@uniklinik-freiburg.de.

0091-6749/$36.00

http://dx.doi.org/10.1016/j.jaci.2012.11.050

Abbreviations used
APC: Allophycocyanin
BAFF-R: B cell–activating factor receptor
BCL10: B-cell lymphoma 10
BCR: B-cell receptor
CARD11: Caspase recruitment domain family, member 11
CD40L: CD40 ligand
CID: Combined immunodeficiency
ERK: Extracellular signal-regulated kinase
FITC: Fluorescein isothiocyanate
GC: Germinal center
gDNA: Genomic DNA
ICOS: Inducible T-cell costimulator
KREC: κ-Deleted receptor excision circle
MALT1: Mucosa associated lymphoid tissue lymphoma translocation gene 1
NF-κB: Nuclear factor κB
NK: Natural killer
pCID: Profound combined immunodeficiency disorder
PE: Phycoerythrin
PerCP: Peridinin-chlorophyll-protein complex
PMA: Phorbol 12-myristate 13-acetate
TCR: T-cell receptor
TREC: T-cell receptor excision circle
Treg: Regulatory T

Caspase recruitment domain family, member 11 (CARD11), belongs to the family of membrane-associated guanylate kinases, which play a crucial role in the differentiation of both neuronal and immunologic tissues as scaffold proteins, facilitating the assembly of clusters of signaling molecules at sites of cell-cell contact.[9] Through its interaction with B-cell lymphoma 10 (BCL10) and mucosa associated lymphoid tissue lymphoma translocation gene 1 (MALT1), CARD11 is essential in the activation of the canonical nuclear factor κB (NF-κB) pathway in lymphocytes.[10] In mice with a targeted deletion of *Card11* or carrying a hypomorphic allele, the antigen-independent development of T and B cells in thymus and bone marrow, respectively, was normal, but peripheral activation–dependent proliferation and differentiation of lymphocytes were altered.[10,11] Serum immunoglobulin levels were low, and after vaccination, *Card11* mutant mice mounted only poor responses to T-dependent and T-independent antigens.[10]

Here we report a female patient with a homozygous deletion of exon 21 in *CARD11* presenting at the age of 13 months with disturbed B-cell differentiation, hypogammaglobulinemia, and *Pneumocystis jirovecii* pneumonia.

METHODS

All investigations were performed after informed consent was granted by the parents. The study was approved by the institutional review board (ITB 0306-10-HMO), according to the declaration of Helsinki. All animal studies were approved by the animal experimentation ethics committee of the Australian National University. For additional information, see the Methods section in this article's Online Repository at www.jacionline.org.

Signaling assays

For detection of phosphorylated p65 and IκBα, PBMCs were incubated for 2 hours at 37°C. Cells were either left untreated or stimulated with 20 μg/mL $F(ab')_2$ anti-IgM (SouthernBiotech, Birmingham, Ala) for 35 minutes and with 200 ng/mL phorbol 12-myristate 13-acetate (PMA; Sigma, St Louis, Mo) or recombinant CD40 ligand (CD40L) for 15 minutes at 37°C.

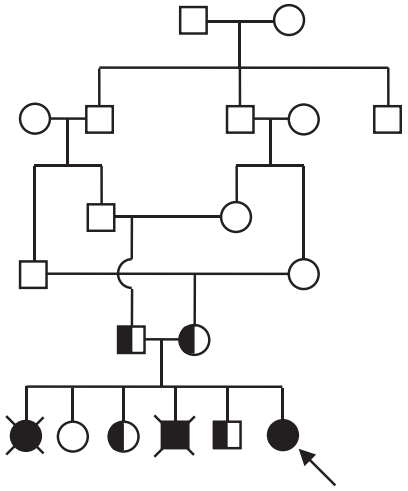

FIG 1. Pedigree of the CARD11-deficient family. *Circles*, Female subjects; *squares*, male subjects; *solid symbols*, homozygous subjects; *half-solid symbols*, heterozygous subjects; *crossed-out symbols*, deceased subjects. The pedigree shows 5 generations of the family. The *arrow* indicates the index patient.

Phosphorylation of extracellular signal-regulated kinase (ERK) 1/2 was determined on stimulation with 20 μg/mL $F(ab')_2$ anti-IgM or 200 ng/mL PMA for 5 minutes at 37°C. Fixation and permeabilization were performed with the BD Biosciences Phosflow intracellular staining kit (BD Biosciences, San Jose, Calif), according to the manufacturer's instructions. Subsequently, cells were stained with antibodies against cell-surface markers and intracellular proteins and analyzed by using flow cytometry.

Intracellular calcium mobilization was measured, as described previously.[12] PBMCs (2×10^6) were labeled with Indo-1 (Invitrogen, Carlsbad, Calif). Subsequent cell-surface staining allowed gating on $CD27^-IgG^-IgA^-$ nonmemory B cells. Baseline acquisition for 45 seconds was followed by stimulation with 10 μg/mL $F(ab')_2$ anti-IgM. Ionomycin (Sigma) was added after 8 minutes as a loading control.

Determination of intracellular cytokines

For determination of intracellular cytokines, a BD staining kit for intracellular cytokines was used, according to the manufacturer's instructions. IL-2 production was detected after stimulation of PBMCs with 100 ng/mL PMA and 0.75 μg/mL ionomycin in the presence of the protein transport inhibitor GolgiStop (BD Biosciences) for 13 hours at 37°C. IL-17, IL-4, and IFN-γ were detected after stimulation of cells with PMA (50 ng/μL) and 1 μg/mL ionomycin for 4 hours at 37°C in the presence of 500 U/mL IL-2 and GolgiPlug. Subsequent to the stimulation, cell-surface staining was performed. Cells were fixed and permeabilized, according to the manufacturer's instructions, and stained for intracellular cytokines.

Activation assays

In vitro stimulation of 5×10^5 PBMCs with 15 μg/mL $F(ab')_2$ anti-IgM and optimal amounts of recombinant CD40L was performed to determine upregulation of activation markers on B cells. Cells were harvested after 2 days and stained with the corresponding antibodies.

T cells (5×10^5) were separated and immediately stimulated through CD3/CD28 beads for 18 hours at 37°C (Invitrogen) to investigate T cell–specific upregulation of activation markers. For activation of mouse T cells, 1.5×10^5 splenocytes were cultured for 18 hours in 96-well plates precoated with 1 μg/mL anti-CD3 or 1 μg/mL anti-CD3 and 10 μg/mL anti-CD28 (all from BD PharMingen). Subsequent to stimulation, cells were washed and stained with the appropriate antibodies.

Plasmablast differentiation

PBMCs of the patient and human cord blood cells (6.25×10^5 cells) were stimulated with CD40L and IL-21 for 9 days in Iscove medium supplemented

TABLE I. Peripheral lymphocyte subpopulations

	Cells/μL	Normal values, cells/μL	Percentage of parental population	Normal values (%)
Leukocytes	7,700	7,400-14,300*		
Lymphocytes	4,900	1,400-12,100†	63.6	43.0-65.2*
CD4 T cells	2,092	400-7,200	42.7	16-91†
Naive cells	1,919	200-7,500	91.7	56-100†
Total memory cells	173	1-650	8.3	0.09-40†
Recent thymic emigrants	1,431	170-7,400	68.4	40-100†
Treg cells	14	20-77	0.65	6-13†
CD8 T cells	1,181	200-2,800	24.1	7-40†
Naive cells	859	30-3,100	72.7	10-100†
Central memory cells	18	5-110	1.5	1-8†
Effector memory cells	2	16-63	1.4	2-100†
Terminally differentiated effector cells	2	55-460	0.1	8-71†
γδ T cells‡			10.1	<10‖
Double-negative T cells§			1.45	<2.5‖
NK T cells‡			0.044	>0.01‖
B cells	990	871-1,553	20.2	16.3-26.8*
Transitional cells	576	109-278	58.2	9.7-17.9*
Naive cells	363	586-955	36.7	61.5-68.7*
IgG-switched cells	8	13-55	0.83	1.5-4.2*
IgA-switched cells	0	8-20	0.01	0.8-1.7*
IgM memory cells	34	40-177	3.41	4.6-15.0*
NK cells	217	55-4,000	4.42	1-96†

Patient's absolute and relative counts of lymphocyte subpopulations are indicated. Percentage refers to the respective parental population. Age-matched reference values are taken from *van Gent et al,[14] †Schatorje et al,[15] or are ‖internal reference values.
‡Percentage of $CD3^+$ T cells.
§Percentage of $CD3^+$ αβ T cells.

with 10% FCS, 1 μg/mL insulin, 2.5 μg/mL apotransferrin, 0.1% fatty acid supplement, 1% nonessential amino acids, 2 mmol/L glutamine, and 1 μg/mL reduced glutathione. CD40L and IL-21 were prepared, as previously described.[13] The phenotype was determined by using flow cytometry.

Immunoglobulin concentrations

Immunoglobulin concentrations were determined by using a sandwich ELISA. In brief, 96-well plates were coated with anti-human Igmix (Jackson ImmunoResearch Laboratories, West Grove, Pa) in bicarbonate buffer. Bound immunoglobulins were detected by using alkaline phosphatase–conjugated anti-human IgM, IgG, or IgA (Jackson ImmunoResearch Laboratories), respectively. Immunoglobulin concentrations were calculated from human IgM, IgG, or IgA standards (N Protein Standard SL; Siemens, Munich, Germany) processed in parallel.

T-cell proliferation

PBMCs were labeled with 0.5 μmol/L carboxyfluorescein diacetate succinimidyl ester (Invitrogen), according to standard protocols. Cells were left untreated or stimulated with 1 μg/mL anti-CD3 (OKT-3; eBioscience, San Diego, Calif) and 1 μg/mL anti-CD28 (BD Biosciences) or 2.5 μg/mL PHA (Remel, Shawnee Mission, Kan) for 5 days at 37°C. Cells were harvested, stained for CD4 and CD8, and subsequently analyzed on a Navios flow cytometer (Beckman Coulter, Fullerton, Calif).

Mouse strain

The unmodulated mouse strain carrying a hypomorphic allele of *Card11* has been described previously.[10] All mice were on a C57BL/6 or B10.BR background.

RESULTS

Case report

At first presentation, we evaluated a 9-month-old girl born to consanguineous parents of Palestinian descent with an upper respiratory tract infection, hypogammaglobulinemia, and a remarkable family history (Fig 1). She is the youngest of 6 children. The firstborn sister failed to thrive and died without diagnosis at 3 months of age because of progressive respiratory failure. The fourth child (male) presented at 6 months of age with meningitis and recurrent pneumonias. At 15 months, he had progressive respiratory distress with high fever and died within a few days. The only recorded laboratory anomaly was a panhypogammaglobulinemia. Three other siblings are healthy with normal immunoglobulin levels. The index patient had a normal medical history until the age of 6 months, when she had an upper respiratory tract infection. At that time, her laboratory examinations revealed significantly reduced IgG levels (IgG, 0.88 g/L; normal range for age, 2.17-9 g/L) but normal IgA (0.35 g/L; normal range for age, 0.11-1.06 g/L) and IgM (0.65 g/L; normal range for age, 0.35-1.26 g/L) levels. Three months later, laboratory tests demonstrated panhypogammaglobulinemia but an otherwise normal immune phenotype, PHA proliferative response, T-cell receptor excision circle (TREC) copy number (5255 copies per 0.5 μg of DNA; normal for age, >400 copies), and T-cell repertoire. She was started on monthly infusions of intravenous immunoglobulins. At the age of 13 months, she presented with fever and severe dyspnea caused by *P jirovecii* pneumonia. After successful treatment, the patient was started on prophylaxis with trimethoprim-sulfamethoxazole, and because of the suspicion of pCID, she was listed for allogeneic bone marrow transplantation. In parallel, a genetic diagnosis made by means of whole-exome sequencing and a single nucleotide polymorphism array was sought.

Immune phenotype of CARD11 deficiency

White blood cell counts at the time of the immunologic characterization were still unremarkable (Table I).[14,15] Flow cytometric analysis of PBMCs depicted normal total CD4 T-cell

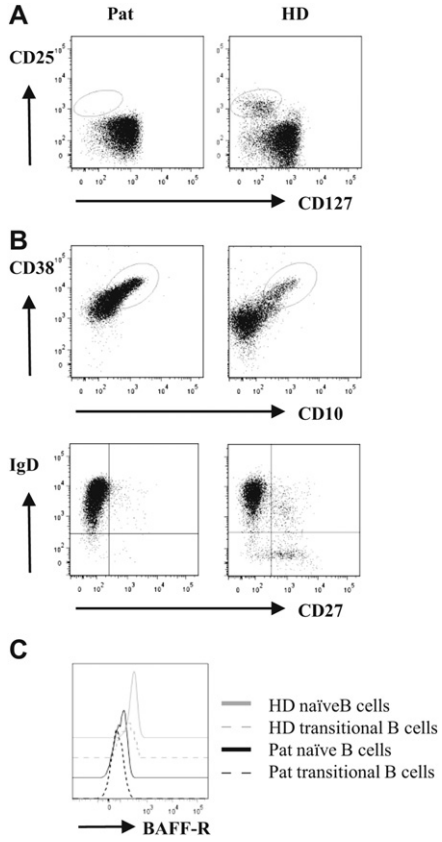

FIG 2. Abnormal lymphocyte homeostasis in CARD11 deficiency. **A** and **B,** $CD127^{-}CD25^{hi}$ Treg cells gated on $CD4^{+}CD3^{+}$ lymphocytes (Fig 2, *A*) and $CD38^{high}CD10^{+}$ transitional B cells *(top)* and CD27/IgD expression gated on $CD19^{+}$ lymphocytes (*bottom*; Fig 2, *B*) of the patient *(Pat)* compared with an age-matched control subject *(HD)*. **C,** BAFF-R expression on the indicated subpopulations.

counts; $CD45RA^{+}$ naive and $CD45RO^{+}$ memory CD4 T cells; and $CD45RA^{+}CD31^{+}$ recent thymic emigrants.[15] However, the absolute and relative counts of regulatory T (Treg) cells ($CD4^{+}CD25^{+}CD127^{-}$) were reduced compared with age-matched reference values (Fig 2, *A*).

Among CD8 T cells, absolute numbers and distribution of naive ($CD27^{+}CD45RA^{+}CCD7^{+}$) and central memory ($CD27^{+}CD45RA^{-}CCD7^{+}$) cells were within the normal range. Effector memory ($CD27^{-}CD45RA^{-}CCD7^{-}$) and terminally differentiated ($CD27^{-}CD45RA^{+}CCD7^{-}$) T-cell counts were reduced according to age-matched reference values in the literature.[15] Also, numbers of natural killer (NK) T cells and CD4/CD8 double-negative α/β T cells were normal; only 10.1% γ/δ T cells was slightly greater than the normal range.

In contrast to the T-cell compartment, the distribution of the patient's B-cell subpopulations was strongly distorted (Table I). Total $CD19^{+}$ B cells were normal in absolute and relative numbers compatible with the previous κ-deleted receptor excision circle (KREC) analysis (4411 copies per 0.5 μg of DNA; normal for age, >1000 copies). The analysis of subpopulations revealed a striking expansion of transitional $CD10^{+}CD38^{hi}IgD^{+}$ B cells, whereas all subsequent populations were reduced compared with age-matched reference values (Fig 2, *B*).[14] Interestingly, B cell–activating factor receptor (BAFF-R) expression was decreased on naive ($CD10^{-}CD38^{+}IgD^{+}$) and transitional B cells of the patient compared with the corresponding subpopulations in an age-matched control subject (Fig 2, *C*).

$CD3^{-}CD16CD56^{+}$ NK cell numbers were normal (Table I). Both $CD56^{bright}CD16^{-}$ and $CD56^{dim}CD16^{+}$ subpopulations were present.

Molecular characterization of CARD11 deficiency

On the basis of parental consanguinity, we assumed a founder mutation transmitted in an autosomal-recessive manner. The DNA single nucleotide polymorphism array resulted in the identification of multiple homozygous regions comprising thousands of genes. We therefore opted for whole-exome sequencing in the patient's DNA sample. While analyzing our data, we heard of a child with a similar phenotype and a mutation in *CARD11* (Greil et al, unpublished data). Comparing uncovered exons in several same-batch exome analyses, we noted that exon 21 of *CARD11* was entirely uncovered in the patient sample but was well covered (approximately ×65) in the control samples.

With *CARD11* as a good candidate, we first sequenced cDNA from the patient with *CARD11*-specific primers. Fragments, including exon 21, were approximately 140 bp shorter than the expected size (Fig 3, *A*). Sanger sequencing of these PCR products revealed a complete lack of exon 21 (136 bp) in the patient's cDNA sequence. All cDNA PCR products without exon 21 were normal in size and sequence. Sequencing genomic DNA (gDNA) between exons 20 and 22 in the patient detected a homozygous 1377-bp genomic deletion, including the entire sequence for exon 21 (Fig 3, *B*). Interestingly, the deletion was flanked by a stretch of 36 completely identical bases. Both parents and 2 healthy siblings were tested heterozygous for this large deletion.

Although CARD11 protein expression was readily detectable in EBV lines of control subjects, no protein could be detected in the patient's EBV line (Fig 3, *C*). Because the antibody was targeted against the N-terminal amino acid 1-221, the deletion of exon 21, encoding amino acid 902-946, must result in a complete loss of CARD11 protein expression.

Signaling in CARD11-deficient T and B cells

The integrity of the canonical NF-κB signaling pathway was addressed by measuring the degradation of IκBα and the phosphorylation of p65 after stimulation of PBMCs with anti-IgM, CD40L, and PMA, respectively.

Strikingly, degradation of IκBα and phosphorylation of p65 after anti-IgM and PMA stimulation, as seen in B cells of healthy donors, was completely absent in the patient's B cells. In contrast, stimulation with CD40L induced degradation of IκBα and phosphorylation of p65 comparable with that seen in the healthy control subject (Fig 4, *A*).

In line with this, we observed an abolished phosphorylation of p65 and degradation of IκBα in the patient's T cells after PMA stimulation, confirming the nonredundant critical role of CARD11 in protein kinase C–dependent signaling in B and T cells (Fig 4, *B*). Given the complex interactions of the diverse signaling pathways downstream of the antigen receptor, we also examined the integrity of other pathways. Anti-IgM and PMA stimulation resulted in normal phosphorylation of ERK1/2 in the patient's B cells (Fig 4, *C*). The same was true for T cells after PMA treatment (Fig 4, *D*), confirming data from mice that this signaling pathway is not affected by the deletion of CARD11.

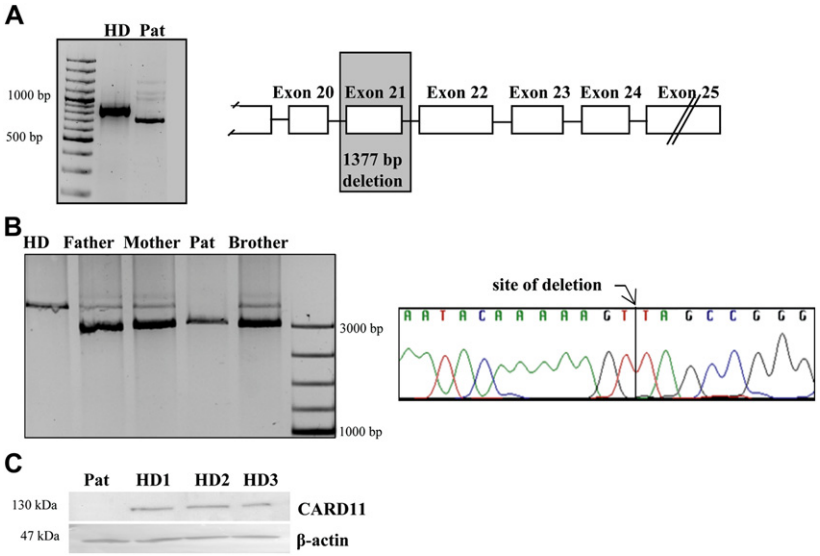

FIG 3. Molecular analysis of CARD11 deficiency. **A,** RT-PCR covering cDNA of exons 16-22 of *CARD11 (left)* and schematic representation of the deletion in *CARD11*, as depicted by the *gray shaded box (right)*. **B,** PCR products amplified from gDNA flanking exon 21 of *CARD11* of a healthy donor *(HD)*, the patient's father and mother, the patient *(Pat)*, and the patient's brother *(left)*. Sanger sequencing of the gDNA including exon 21 of *CARD11 (right)*. **C,** Immunoblot for CARD11 protein expression in EBV lines of the patient and 3 control subjects. β-Actin was used as a loading control.

Also, calcium mobilization in B cells after anti-IgM stimulation was undistinguishable from that seen in healthy control cells (Fig 4, *E*).

B-cell function in the patient with CARD11 deficiency

On stimulation for 48 hours through the BCR, expression of intercellular adhesion molecule 1 and CD25 was not induced in the patient's B cells, whereas stimulation of PBMCs with CD40L resulted in a comparable upregulation of both activation markers in the patient's and control subject's B cells, confirming their dependence on NF-κB on BCR stimulation. The regular upregulation of CD69 and CD86 on stimulation with anti-IgM and CD40L excluded an overall activation defect (Fig 5, *A*).

In addition, the patient's B cells developed into plasmablasts after stimulation with CD40L and IL-21, which is comparable with what was seen in cells from human cord blood (Fig 5, *B*), demonstrating the capacity of terminal B-cell differentiation despite CARD11 deficiency. Moreover, CARD11-deficient plasmablasts produced similar amounts of IgG and IgA *in vitro*, which was comparable with those seen in cord blood control samples, whereas IgM levels were increased (Fig 5, *C*).

T-cell and NK-cell function in CARD11 deficiency

To investigate the effect of CARD11 deficiency on cytokine production and activation, we determined IL-2, IL-4, IFN-γ, and IL-17 production after stimulation with PMA/ionomycin. Although the percentages of IL-2–, IL-17–, and IFN-γ–producing CD4 T cells were reduced compared with those seen in control subjects, IL-4–producing CARD11-deficient CD4 T cells were within the normal range (Fig 6, *A*). Upregulation of CD69, CD25, CD40L, OX40, and inducible T-cell costimulator (ICOS) was determined on CD4 T cells (Fig 6, *B*). After TCR/CD28 stimulation, CD69 and CD40L upregulation was within normal ranges, whereas the increase in OX40, CD25, and ICOS expression was strongly impaired in CARD11-deficient CD4 T cells compared with that seen in healthy control subjects. Finally, proliferation of CARD11-deficient CD4 T cells after CD3/CD28 stimulation was completely abrogated *in vitro*, whereas CD4 T cells proliferated after stimulation with PHA, although slightly less than in control PBMCs (Fig 6, *C*). Equivalent results were observed for CD8 T cells (data not shown).

After PMA/ionomycin stimulation of PBMCs, less NK cells produced IFN-γ in the setting of CARD11 deficiency (Fig 6, *D*).

Defective Baff-R expression and upregulation of activation markers in murine CARD11 deficiency

Proposing a crucial role of CARD11 in early peripheral B-cell differentiation and germinal center (GC) induction through ICOS, we went back to our Card11 mutant mouse model.[10] In these mice both mature and immature B-cell subsets expressed lower levels of Baff-R, most strongly affecting the T2 transitional B-cell stage (Fig 7, *A*).

Because the upregulation of most costimulatory molecules on murine Card11-deficient T cells after anti-CD3/CD28 activation had not been described previously, we investigated the upregulation of CD69, CD25, CD40L, Ox40, and Icos in Card11 mutant mice compared with that seen in control littermates. T cells from naive Card11 mutant mice showed impaired upregulation of all determined activation markers, especially in response to anti-CD3/CD28 stimulation, rendering the severe deficiency in upregulation of costimulatory molecules a key contributing factor to the disturbed T-dependent responses in Card11 deficiency (Fig 7, *B*).

DISCUSSION

Here we report the case of a child with a new form of profound combined immunodeficiency caused by a homozygous deletion

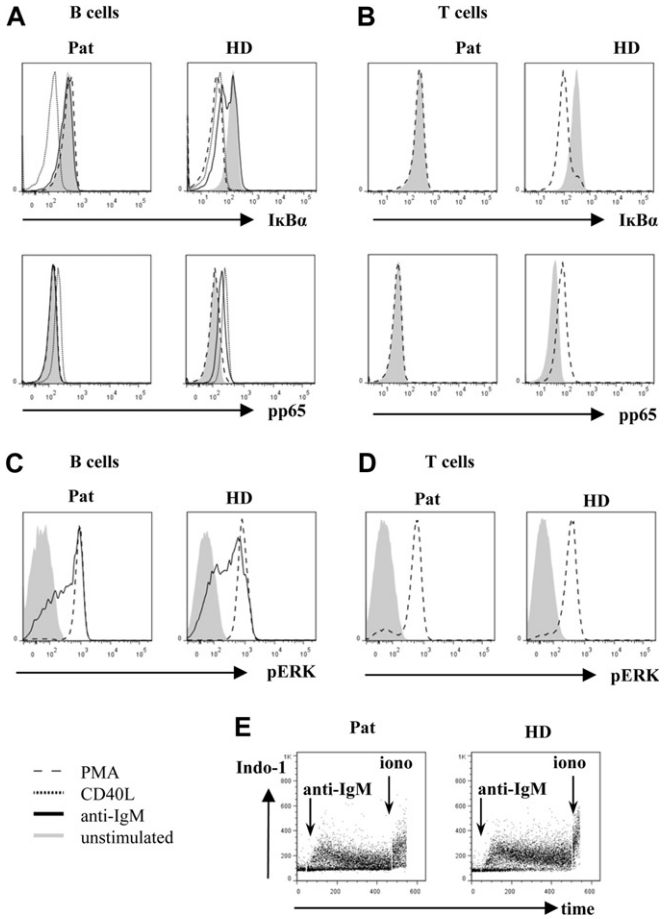

FIG 4. Signaling in CARD11-deficient lymphocytes. **A,** Degradation of IκBα *(upper panels)* and phosphorylation of p65 (pp65, *lower panels*) gated on $CD19^+$ B cells on stimulation, as indicated. **B,** Degradation of IκBα *(upper panels)* and phosphorylation of p65 *(lower panels)* on stimulation of PBMCs with PMA *(dashed line)* and unstimulated conditions gated on $CD3^+$ T cells. **C,** Phosphorylation of ERK1/2 *(pERK)* in $CD19^+$ B cells after stimulation. **D,** Phosphorylation of ERK in $CD3^+$ T cells after stimulation with PMA and unstimulated. **E,** Calcium mobilization in $CD19^+CD27^+IgG^-IgA^-$ B cells on anti-IgM stimulation. Depicted is the bound/unbound Indo-1 ratio. *Arrows* indicate time points of the addition of anti-IgM and ionomycin. *HD*, Healthy donor; *Pat*, patient.

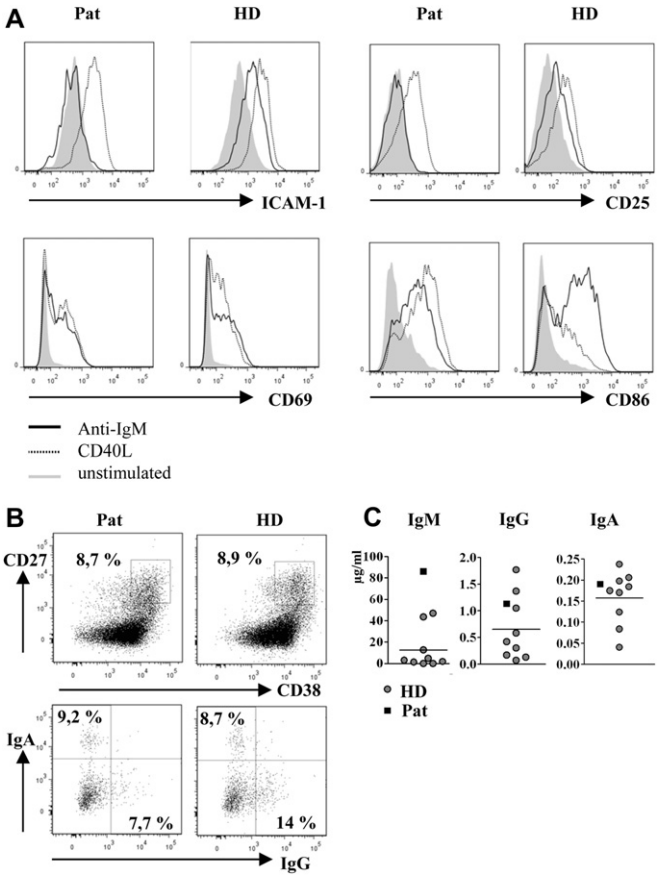

FIG 5. B-cell function in CARD11 deficiency. **A,** Intercellular adhesion molecule 1 *(ICAM-1)*, CD25, CD69, and CD86 expression after stimulation of PBMCs gated on $CD19^+$ cells. **B,** Differentiation of plasmablasts, defined as $CD38^{hi}CD27^{hi}$ B cells, after *in vitro* stimulation of PBMCs with IL-21 and CD40L *(upper panel)*. IgG^+ and IgA^+ plasmablasts are depicted after gating on $CD38^{hi}CD27^{hi}$ B cells *(lower panel)*. **C,** IgM, IgG, and IgA levels from cell-culture supernatants of the patient's PBMCs or cord blood after *in vitro* stimulation with IL-21 and CD40L. *HD*, Healthy donor; *Pat*, patient.

in *CARD11*. The manifestation of the first opportunistic infection in the context of hypogammaglobulinemia, consanguinity, and a positive family history prompted a genomic screening for a causal defect. This search was significantly accelerated with the finding of CARD11 deficiency in a second child by Greil et al (unpublished data). These 2 children demonstrate that complete CARD11 deficiency presents rather early in life with pCID and not with common variable immunodeficiency, as had been suspected and previously tested unsuccessfully.[16]

From a clinical standpoint, it is important to notice that pCID in the setting of CARD11 deficiency will be missed by testing for TREC/KREC copy numbers during newborn screening and by checking lymphocyte counts later in life because numbers of T, B, and NK cells might be normal, as in our child. The essential diagnostic clues are as follows: missing T-cell proliferation to anti-CD3/CD28 stimulation and abnormal expansion of late transitional B cells, lack of mature B cells, and hypogammaglobulinemia. *Card11*-targeted mouse strains demonstrated that the defective activation of NF-κB and c-Jun N-terminal kinase after antigen receptor and PMA stimulation is the responsible pathomechanism in patients with CARD11 deficiency.[10,17-19] Similarly, we found defective canonical NF-κB activation and intact ERK and calcium activation in the B and T cells of our patient, endorsing the selective effect of human CARD11 deficiency on the antigen receptor pathway.

Despite severely disturbed proliferation after TCR stimulation, the differentiation of peripheral T-cell subpopulations is normal, except for Treg cells.[20,21] The differentiation and maintenance of Treg cells depend on proper IL-2 signals.[22,23] We could demonstrate that CARD11-deficient T cells did not produce normal amounts of IL-2 and upregulation of the IL-2 receptor α chain (CD25) after TCR stimulation was diminished. Thus reduced IL-2 production and IL-2 receptor expression might contribute to Treg cell deficiency in human subjects in addition to the previously demonstrated direct role of CARD11 in IL-2 receptor signaling.[23] IFN-γ production was more strongly affected than IL-4 production in the T cells of our patient. This is in contrast to recent reports in mice demonstrating a crucial role of CARD11 in T_H2 cell differentiation.[24] Interestingly, also IL-17 was severely reduced, demonstrating a complex dysregulation

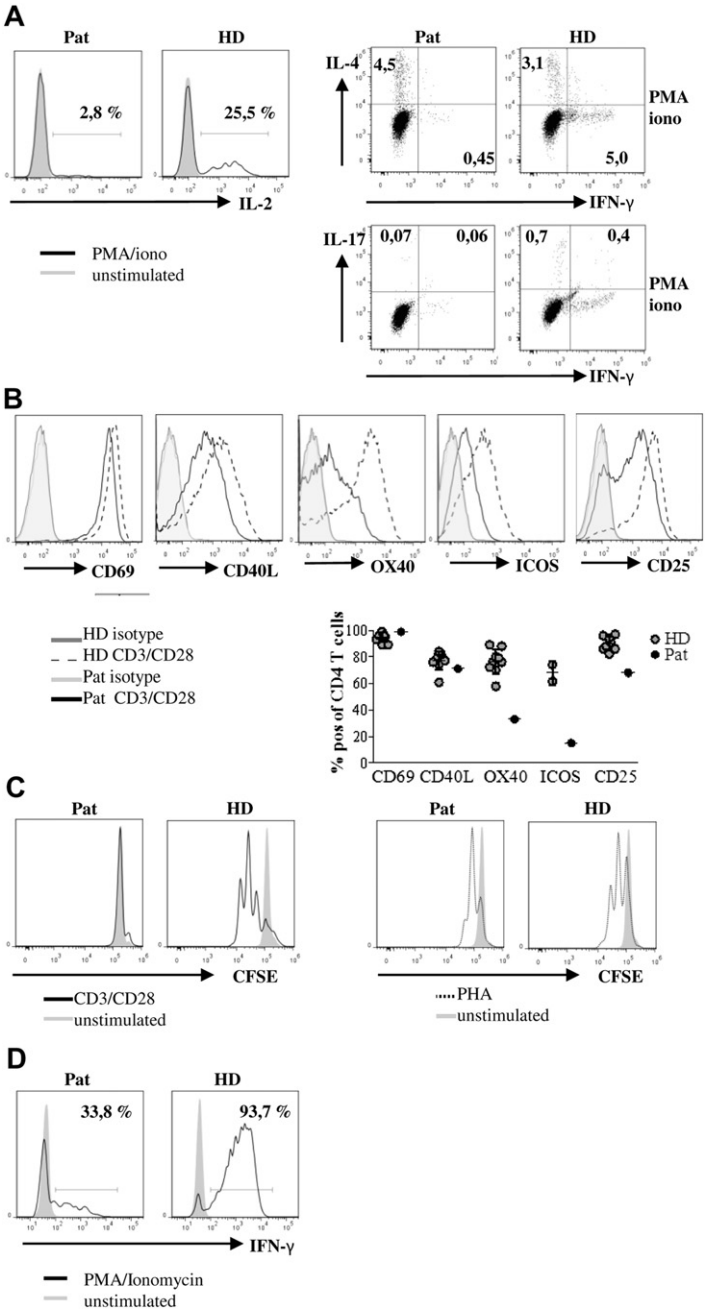

FIG 6. T-cell and NK cell function in CARD11 deficiency. **A,** PBMCs were stimulated with PMA/ionomycin to determine IL-2 *(upper left)*, IL-4, and IFN-γ production *(upper right)* and IL-17 and IFN-γ production *(lower right)* on $CD4^+$ T cells. **B,** Expression of CD69, CD40L, OX40, ICOS, and CD25 after stimulation of $CD4^+$ T cells, as indicated *(top)*. The percentage of positive cells for indicated markers of $CD4^+$ T cells of the patient *(open circles)* compared with healthy control subjects (*closed circles*, *bottom*). **C,** Proliferation of $CD4^+$ T cells on stimulation with anti-CD3/anti-CD28 *(left)* and PHA *(right)*. **D,** IFN-γ production in $CD3^-CD56^+$ NK cells after stimulation with PMA/ionomycin compared with unstimulated samples. *HD*, Healthy donor; *Pat*, patient.

of the effector function of the T-cell compartment. It remains speculative whether this functional defect contributed to the susceptibility to *P jirovecii* infection in our patient because IFN-γ and IL-17 are supposedly involved in the defense against *P jirovecii* infection.[25] Regarding NK cell differentiation, NJ cell numbers seem to depend on the genetic background of the mouse model.[17,21,26] In accordance with the report by Malarkannan et al[27] that the CARD11/MALT1/bcl10 complex is involved in NF-κB–dependent cytokine production in NK cells but does not affect their differentiation, we observed normal NK cell numbers, a regular distribution of subsets, but markedly decreased production of IFN-γ by the patient's NK cells.

Most striking are the changes in the B-cell compartment. We observed a severe developmental block at the IgD^+IgM^{hi} late

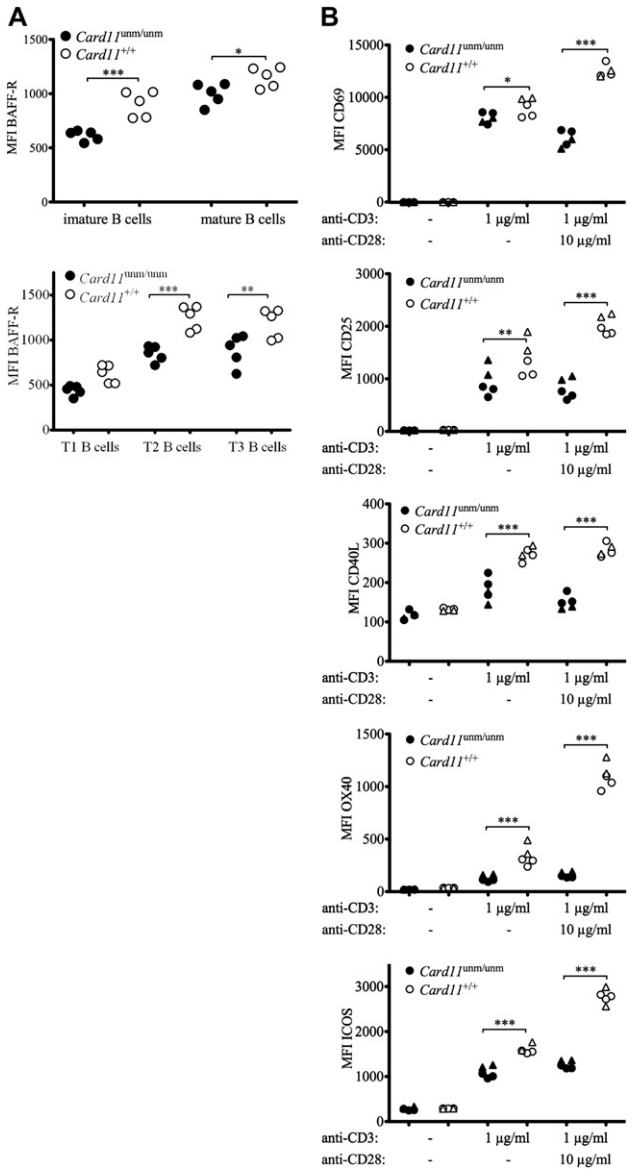

FIG 7. Expression of Baff-R and T-cell activation markers in *Card11* mutant mice. **A,** Expression of Baff-R on $CD93^+$ immature and $CD93^-$ mature splenic B cells from *Card11*$^{unm/unm}$ mice and age-matched control animals *(top panel)*. After staining for IgM and CD23, the $CD93^+$ immature B cells were further divided into T1 (IgM^+CD23^-), T2 (IgM^+CD23^+), and T3 ($IgM^{low}CD23^+$) stages *(bottom panel)*. **B,** Expression of CD69, CD25, CD40L, Ox40, and Icos on 7-amino-actinomycin D-negative $CD4^+$ T cells after stimulation, as indicated. *Triangles*, Mice from a C57BL/6 background; *circles*, mice from a B10.BR background. Statistical analysis was done with ANOVA, followed by the Bonferroni post-test. *MFI*, Mean fluorescence intensity. $*P < .05$, $**P < .005$, and $***P < .0005$.

transitional B-cell stage affecting all mature B-cell subpopulations in the setting of CARD11 deficiency. In accordance, all mouse models demonstrated a reduction in mature B-cell numbers.[10,17] This finding was corroborated by the defective B-cell differentiation seen in mice with targeted deletion of the other members of the CARD11/MALT1/bcl10 complex.[28,29] The exact reason for this developmental block remains unknown. In addition to the BCR signal, B cells depend on BAFF-R expression and signaling at this stage. Thus also BAFF-R-deficient mice and human subjects have a block at the transitional stage, and mature B-cell numbers are severely reduced.[13,30,31] Because the alternative NF-κB pathway downstream of BAFF-R is independent of CARD11 and BAFF-R itself is a potential NF-κB target gene,[32] we speculated about a reduced BAFF-R expression on CARD11-deficient B cells. Indeed, CARD11-deficient B cells did not express normal amounts of BAFF-R on the surface. Whole-exome sequencing excluded any mutations in BAFF-R itself, and the analysis of CARD11-deficient murine B cells confirmed this finding. Therefore in addition to the disturbed BCR signal, low BAFF-R expression might contribute to the disturbed B-cell differentiation beyond the late transitional stage in human CARD11 deficiency. This seems to differ from mice, in which the developmental block at the transitional stage is less prominent,[10] despite reduced BAFF-R expression. This aspect needs to be revisited more carefully in the different murine models.

The crucial defect in late B-cell differentiation leading to reduced serum immunoglobulin levels and defective T-dependent and T-independent immune responses was common to all mouse models.[10,17-19] Jun et al[10] additionally described poor GC formation. Similarly, Malt1- and bcl10-deficient mice show insufficient formation of GC B cells after immunization with T-dependent antigens.[33] Again, it remains unknown which mechanisms contribute to the failure of GC formation. Interestingly, in addition to the reduced induction of OX40 and CD25, we found a severe defect in the upregulation of ICOS after TCR activation and confirmed it in our mouse model. In contrast to the globally affected upregulation of activation markers in CARD11-deficient murine T cells, CD40L induction on the patient's T cells was still within the normal range. Given the essential role of ICOS in GC formation in mice and human subjects,[34-38] it is very tempting to speculate that impaired ICOS upregulation plays an important role in poor B-cell memory formation in human CARD11 deficiency.

Although hypogammaglobulinemia is a common finding in all reports of CARD11 deficiency, our data reveal that differentiation of plasmablasts is not completely dependent on CARD11 expression because CD40L/IL-21 stimulation allowed efficient generation of plasmablast differentiation and immunoglobulin production *in vitro*. In this context, it is noteworthy that CD40 activation of the canonical NF-κB pathway was normal, and therefore CD40-induced B-cell activation is independent of CARD11, which is in contrast to early reports.[18]

In the case of our patient, because of the severe clinical presentation, it was decided to proceed to allogeneic bone marrow transplantation from her fully matched heterozygous brother. She underwent successful transplantation and has full donor chimerism and normal immunoglobulin levels without evidence of graft-versus-host disease 5 months later.

In summary, we have discovered a new form of pCID caused by a genetic deletion in *CARD11*. The described genetic recombination between homologous regions upstream and downstream of exon 21 suggests a potential hot-spot mutation in this gene for which screening in a larger cohort of patients with pCIDs is worthwhile. In the absence of lymphopenia, the diagnostic clues in CARD11 deficiency derive from abnormal B-cell differentiation and absent T-cell proliferation after TCR/CD28 stimulation. Signaling studies reveal defective canonical NF-κB activation after antigen receptor but not CD40 stimulation. CARD11 is a crucial scaffold of the adaptive immune system controlling peripheral B-cell differentiation, a variety of critical T-cell effector functions, and the GC response. The restricted expression of CARD11 in the hematopoietic system makes patients with

CARD11 deficiency excellent candidates for stem cell transplantation.

We thank the patient and her parents for their support, Mehmet Yabas for FACS measurement, and J. Hodges and B. Roller for critical reading of the manuscript.

Clinical implications: CARD11 deficiency presents as combined immunodeficiency despite normal lymphocyte counts. Diagnostic clues are hypogammaglobulinemia, B-cell phenotype, and lack of T-cell proliferation to anti-CD3/CD28. The immunodeficiency can be successfully corrected by using hematopoietic stem cell transplantation.

REFERENCES

1. van der Burg M, Gennery AR. Educational paper. The expanding clinical and immunological spectrum of severe combined immunodeficiency. Eur J Pediatr 2011; 170:561-71.
2. Al-Herz W, Bousfiha A, Casanova J-L, Chapel H, Conley ME, Cunningham-Rundles C, et al. Primary Immunodeficiency Diseases: an update on the Classification from the International Union of Immunological Societies Expert Committee for Primary Immunodeficiency. Front Immunol 2011;2:54.
3. Arnaiz-Villena A, Timon M, Corell A, Perez-Aciego P, Martin-Villa JM, Regueiro JR. Brief report: primary immunodeficiency caused by mutations in the gene encoding the CD3-gamma subunit of the T-lymphocyte receptor. N Engl J Med 1992;327:529-33.
4. Feske S, Gwack Y, Prakriya M, Srikanth S, Puppel SH, Tanasa B, et al. A mutation in Orai1 causes immune deficiency by abrogating CRAC channel function. Nature 2006;441:179-85.
5. Picard C, McCarl CA, Papolos A, Khalil S, Luthy K, Hivroz C, et al. STIM1 mutation associated with a syndrome of immunodeficiency and autoimmunity. N Engl J Med 2009;360:1971-80.
6. Elder ME, Hope TJ, Parslow TG, Umetsu DT, Wara DW, Cowan MJ. Severe combined immunodeficiency with absence of peripheral blood CD8+ T cells due to ZAP-70 deficiency. Cell Immunol 1995;165:110-7.
7. Linka RM, Risse SL, Bienemann K, Werner M, Linka Y, Krux F, et al. Loss-of-function mutations within the IL-2 inducible kinase ITK in patients with EBV-associated lymphoproliferative diseases. Leukemia 2012;26:963-71.
8. Li FY, Chaigne-Delalande B, Kanellopoulou C, Davis JC, Matthews HF, Douek DC, et al. Second messenger role for Mg2+ revealed by human T-cell immunodeficiency. Nature 2011;475:471-6.
9. Caruana G. Genetic studies define MAGUK proteins as regulators of epithelial cell polarity. Int J Dev Biol 2002;46:511-8.
10. Jun JE, Wilson LE, Vinuesa CG, Lesage S, Blery M, Miosge LA, et al. Identifying the MAGUK protein Carma-1 as a central regulator of humoral immune responses and atopy by genome-wide mouse mutagenesis. Immunity 2003;18:751-62.
11. Gross O, Grupp C, Steinberg C, Zimmermann S, Strasser D, Hannesschlager N, et al. Multiple ITAM-coupled NK cell receptors engage the Bcl10/Malt1 complex via Carma1 for NFκB and MAPK activation to selectively control cytokine production. Blood 2008;112:2421-8.
12. Foerster C, Voelxen N, Rakhmanov M, Keller B, Gutenberger S, Goldacker S, et al. B cell receptor-mediated calcium signaling is impaired in B lymphocytes of type Ia patients with common variable immunodeficiency. J Immunol 2010;184:7305-13.
13. Warnatz K, Salzer U, Rizzi M, Fischer B, Gutenberger S, Bohm J, et al. B-cell activating factor receptor deficiency is associated with an adult-onset antibody deficiency syndrome in humans. Proc Natl Acad Sci U S A 2009;106:13945-50.
14. van Gent R, van Tilburg CM, Nibbelke EE, Otto SA, Gaiser JF, Janssens-Korpela PL, et al. Refined characterization and reference values of the pediatric T- and B-cell compartments. Clin Immunol 2009;133:95-107.
15. Schatorje EJ, Gemen EF, Driessen GJ, Leuvenink J, van Hout RW, de Vries E. Paediatric reference values for the peripheral T cell compartment. Scand J Immunol 2012;75:436-44.
16. Tampella G, Baronio M, Vitali M, Soresina A, Badolato R, Giliani S, et al. Evaluation of CARMA1/CARD11 and Bob1 as candidate genes in common variable immunodeficiency. J Investig Allergol Clin Immunol 2011;21:348-53.
17. Hara H, Wada T, Bakal C, Kozieradzki I, Suzuki S, Suzuki N, et al. The MAGUK family protein CARD11 is essential for lymphocyte activation. Immunity 2003;18: 763-75.
18. Egawa T, Albrecht B, Favier B, Sunshine MJ, Mirchandani K, O'Brien W, et al. Requirement for CARMA1 in antigen receptor-induced NF-kappa B activation and lymphocyte proliferation. Curr Biol 2003;13:1252-8.
19. Newton K, Dixit VM. Mice lacking the CARD of CARMA1 exhibit defective B lymphocyte development and impaired proliferation of their B and T lymphocytes. Curr Biol 2003;13:1247-51.
20. Medoff BD, Sandall BP, Landry A, Nagahama K, Mizoguchi A, Luster AD, et al. Differential requirement for CARMA1 in agonist-selected T-cell development. Eur J Immunol 2009;39:78-84.
21. Barnes MJ, Krebs P, Harris N, Eidenschenk C, Gonzalez-Quintial R, Arnold CN, et al. Commitment to the regulatory T cell lineage requires CARMA1 in the thymus but not in the periphery. PLoS Biol 2009;7:e51.
22. Malek TR, Castro I. Interleukin-2 receptor signaling: at the interface between tolerance and immunity. Immunity 2010;33:153-65.
23. Lee AJ, Wu X, Cheng H, Zhou X, Cheng X, Sun SC. CARMA1 regulation of regulatory T cell development involves modulation of interleukin-2 receptor signaling. J Biol Chem 2010;285:15696-703.
24. Medoff BD, Seed B, Jackobek R, Zora J, Yang Y, Luster AD, et al. CARMA1 is critical for the development of allergic airway inflammation in a murine model of asthma. J Immunol 2006;176:7272-7.
25. Gigliotti F, Wright TW. Immunopathogenesis of *Pneumocystis carinii* pneumonia. Expert Rev Mol Med 2005;7:1-16.
26. Hara H, Ishihara C, Takeuchi A, Xue L, Morris SW, Penninger JM, et al. Cell type-specific regulation of ITAM-mediated NF-kappaB activation by the adaptors, CARMA1 and CARD9. J Immunol 2008;181:918-30.
27. Malarkannan S, Regunathan J, Chu H, Kutlesa S, Chen Y, Zeng H, et al. Bcl10 plays a divergent role in NK cell-mediated cytotoxicity and cytokine generation. J Immunol 2007;179:3752-62.
28. Ruland J, Duncan GS, Wakeham A, Mak TW. Differential requirement for Malt1 in T and B cell antigen receptor signaling. Immunity 2003;19:749-58.
29. Xue L, Morris SW, Orihuela C, Tuomanen E, Cui X, Wen R, et al. Defective development and function of Bcl10-deficient follicular, marginal zone and B1 B cells. Nat Immunol 2003;4:857-65.
30. Thompson JS, Bixler SA, Qian F, Vora K, Scott ML, Cachero TG, et al. BAFF-R, a newly identified TNF receptor that specifically interacts with BAFF. Science 2001; 293:2108-11.
31. Sasaki Y, Derudder E, Hobeika E, Pelanda R, Reth M, Rajewsky K, et al. Canonical NF-kappaB activity, dispensable for B cell development, replaces BAFF-receptor signals and promotes B cell proliferation upon activation. Immunity 2006;24:729-39.
32. Fu L, Lin-Lee YC, Pham LV, Tamayo A, Yoshimura L, Ford RJ. Constitutive NF-kappaB and NFAT activation leads to stimulation of the BLyS survival pathway in aggressive B-cell lymphomas. Blood 2006;107:4540-8.
33. Tusche MW, Ward LA, Vu F, McCarthy D, Quintela-Fandino M, Ruland J, et al. Differential requirement of MALT1 for BAFF-induced outcomes in B cell subsets. J Exp Med 2009;206:2671-83.
34. Tafuri A, Shahinian A, Bladt F, Yoshinaga SK, Jordana M, Wakeham A, et al. ICOS is essential for effective T-helper-cell responses. Nature 2001;409:105-9.
35. McAdam AJ, Greenwald RJ, Levin MA, Chernova T, Malenkovich N, Ling V, et al. ICOS is critical for CD40-mediated antibody class switching. Nature 2001; 409:102-5.
36. Bossaller L, Burger J, Draeger R, Grimbacher B, Knoth R, Plebani A, et al. ICOS deficiency is associated with a severe reduction of CXCR5+CD4 germinal center Th cells. J Immunol 2006;177:4927-32.
37. Warnatz K, Bossaller L, Salzer U, Skrabl-Baumgartner A, Schwinger W, van der BM, et al. Human ICOS deficiency abrogates the germinal center reaction and provides a monogenic model for common variable immunodeficiency. Blood 2006; 107:3045-52.
38. Dong C, Juedes AE, Temann UA, Shresta S, Allison JP, Ruddle NH, et al. ICOS co-stimulatory receptor is essential for T-cell activation and function. Nature 2001;409:97-101.

METHODS

Cell separation and flow cytometry

PBMCs were separated by means of Ficoll density centrifugation from EDTA blood and cultured in RPMI 1640 (Biochrom, Cambridge, United Kingdom) supplemented with penicillin, streptomycin, and 10% FCS, if not described differently. When necessary, exclusion of dead cells was performed with 4′-6-diamidino-2-phenylindole dihydrochloride (Sigma) or 7-amino-actinomycin D (eBioscience) staining.

Quantification of TRECs and KRECs

TREC and KREC numbers were determined by using quantitative RT-PCR. Reactions in peripheral blood were evaluated with 0.5 μg of gDNA extracted from the patient's PBMCs. PCR reactions contained TaqMan universal PCR master mix (Applied Biosystems, Foster City, Calif), specific primers (900 nmol/L), and FAM-TAMRA probes (250 nmol/L), as previously described.[E1] Quantitative RT-PCR was carried out in an ABI PRISM 7900 Sequence Detector System (Applied Biosystems). Amplification of RNAse P (TaqMan assay, Applied Biosystems) served as a quality control to verify similar amounts of gDNA that were used in the assays for both the TREC and KREC analyses.

Molecular genetics analyses

A search for homozygous regions in the DNA of patient was performed with the Affymetrix GeneChip Human Mapping 250K Nsp Array (Affymetrix, Santa Clara, Calif), as previously described.[E2]

Whole-exome sequencing was performed in DNA from patient 5168 by using the SureSelect Human All Exon v.2 Kit (Agilent Technologies, Santa Clara, Calif) on HiSeq2000 (Illumina, San Diego, Calif) as 100-bp paired-end runs. Image analysis and base calling were performed with the Genome Analyzer Pipeline version 1.5 with default parameters. The reads were aligned with DNAnexus software (Palo Alto, Calif) by using the default parameters with the human genome assembly hg19 (GRCh37) as a reference, as previously described.[E3]

Isolation of RNA was performed from patient and control EBV lines by using the Quick RNA MicroPrep kit, according to the manufacturer's instructions. cDNA was obtained by means of reverse transcription of 100 μg of RNA with Superscript RT II (Invitrogen). Focusing on exons annotated in gDNA in the region of chromosome 7 (2954789-295508) PCR was performed for cDNA of segment exons 16-22 by using the Qiagen Taq Polymerase (Qiagen, Hilden, Germany) with primers as follows: forward, AGCTTCGTGCACTCGGTCAA; reverse, CGGCGCTCGCAGTAGAA. PCR was performed for 35 cycles at an annealing temperature of 58°C for 50 seconds.

gDNA was isolated from whole blood by using standard methods. Primers for PCR were chosen to amplify a 4036-bp product surrounding exon 21 with an annealing temperature of 63°C, as follows: forward, GCCAAGCCCAG CAGGGCCTGACTGATTGAT; reverse, GCAGTAGAAGGCGCGTACCAG GCTGTAGG. The resulting PCR product was sequenced in both directions at an annealing temperature of 63°C by using the Sanger method (BigDye v3.1, ABI 3130xl Genetic Analyzer) with the following primers: forward, GGGA GACTGAGGCG GGTGGATAACTTGAGG; reverse, TCCCACCTCAGCC TCCCAAGTGGCTGG.

Immunoblotting

Fifty-microgram whole-cell lysates of EBV-transformed cell lines of the patient and 2 healthy control subjects were separated by using SDS gel electrophoresis. CARD11 was detected with a polyclonal rabbit anti-human CARD11 antibody, recognizing the C-terminus of the protein (Enzo Life Science, Farmingdale, NY). Polyclonal rabbit anti-human β-actin (Sigma) served as a loading control. For detection of primary antibodies, incubation with horseradish peroxidase–conjugated donkey anti-rabbit antibody (GE Healthcare, Fairfield, Conn) was followed by detection with SuperSignal West Chemiluminescent Substrate (Thermo Scientific, Waltham, Mass).

For flow cytometric staining, the following antibodies were used: anti-IgD fluorescein isothiocyanate (FITC), anti-IgA phycoerythrin (PE; Southern Biotech), anti-IgG FITC (Dako, Glostrup, Denmark), anti-CD45RA FITC, anti-CD10 PE, anti-CD19 PE-Cy7, anti-CD3 PE-Cy7, anti-mouse IgG1 FITC, anti-CD4 PE-Cy7, anti-CD45 Pacific Blue, anti-CD19 Krome Orange (all from Beckman Coulter), anti-CD21 PE, anti-CD4 Pacific Blue, anti-CD31 PE, anti-CD25 peridinin-chlorophyll-protein complex (PerCP)-Cy5.5, anti-CD27 Pacific Blue, anti-CD8 allophycocyanin (APC), anti-CD38 PerCP-Cy5.5, anti-CD127 Alexa Fluor 647, anti-p65(pS529) Alexa Fluor 488 and anti-IκBα PE, anti-ERK1/2(pT202/pY204) Alexa Fluor 647, anti-CD27 APC, anti-CD27 FITC, anti-CD4 APC, anti-mouse IgG1 PE, anti-CD40L PE, anti-OX40 PE, anti-CD69 FITC, anti-CD25 FITC, anti-IgG PE, anti-CD3 PerCP, anti-CD27 PerCP-Cy5.5, anti-IFN-γ FITC, anti-CD86 PE, anti-CD25 PerCP-Cy5.5 anti-CD8 APC (all from BD Biosciences), anti-IgM Cy5, IgA DyLight 649 (Jackson ImmunoResearch), anti-CCR7 PE (R&D Systems, Minneapolis, Minn), anti-CD19 Brilliant violet 421, anti-CD8 Pacific Blue anti–IL-2 PE, CD38 PE-Cy7, CD27 PerCP-Cy5.5 (all from BioLegend, San Diego, Calif), anti-ICOS PE, anti–IL-4 APC and anti–IL-17 PE (all from eBioscience).

For mouse experiments, the following antibodies were used: B220 PerCP, CD40L biotin (both from BD PharMingen), IgM PE-Cy7, CD93 APC, CD8 APC, CD69 PE-Cy7, Icos FITC (all from eBioscience), B220 Alexa Fluor 700, Baff-R PE, CD23 Pacific Blue, CD4 Alexa Fluor 700, Ox40 PE, CD25 APC-Cy7 (all from BioLegend), and Streptavidin Qdots 605 (Invitrogen).

REFERENCES

E1. Lev A, Simon AJ, Bareket M, Bielorai B, Hutt D, Amariglio N, et al. The kinetics of early T and B cell immune recovery after bone marrow transplantation in RAG-2-deficient SCID patients. PLoS One 2012;7:e30494.
E2. Edvardson S, Shaag A, Kolesnikova O, Gomori JM, Tarassov I, Einbinder T, et al. Deleterious mutation in the mitochondrial arginyl-transfer RNA synthetase gene is associated with pontocerebellar hypoplasia. Am J Hum Genet 2007;81:857-62.
E3. Edvardson S, Cinnamon Y, Jalas C, Shaag A, Maayan C, Axelrod FB, et al. Hereditary sensory autonomic neuropathy caused by a mutation in dystonin. Ann Neurol 2012;71:569-72.